Fractionation of BSA and Lysozyme Using Ultrafiltration: Effect of Gas Sparging

Raja Ghosh, Qiangyi Li, and Zhanfeng Cui
Dept. of Engineering Science, University of Oxford, Oxford OX1 3PJ, England

Fractionation of proteins by ultrafiltration is an interesting challenge. With a particular membrane, the protein–protein and protein–membrane interactions largely decide which protein passes through and which is retained. System hydrodynamics also affects protein fractionation as the transmission behavior of a protein is altered by concentration polarization. Therefore, disruption of the concentration polarization layer would help to maintain the native selectivity of the membrane and hence aid in protein fractionation. An attempt is made to use gas sparging, a technique proven effective in controlling concentration polarization to enhance the selectivity of separation of BSA (MW 67,000) and lysozyme (MW 14,100). The effects of gas flow rate, liquid flow rate and feed concentration on the selectivity of fractionation are examined. Gas sparging enhances protein fractionation; under suitable solution conditions, nearly complete separation of BSA and lysozyme was achieved with gas sparged ultrafiltration. The permeate flux was also increased by gas sparing. The mechanism of enhancement is explained in terms of disruption of the concentration polarization layer and enhanced mass transfer due to bubble-induced secondary flow.

Introduction

In recent years, ultrafiltration, a pressure-driven, membrane-based separation process, has emerged as a major bioseparation technique for large-scale purification and polishing of protein products such as therapeutic drugs, enzymes, vaccines, and antibodies, mainly due to its inherently high throughput. However, the major concern with using ultrafiltration (size-based) for protein fractionation is the poor selectivity of solute separation. The lower selectivity, as mentioned by Rodgers and Sparks (1991), is due to the following reasons:

- A broad distribution in membrane pore size
- Protein–protein interactions (aggregation)
- Protein–membrane interaction (adsorption and fouling)
- Concentration polarization (bulk mass-transfer limitation).

Adjustment of solution conditions such as pH and ionic strength can be used to alter protein–protein and protein–membrane interactions in order to achieve a high separation efficiency by ultrafiltration with a specific membrane. Indeed, many researchers have identified the importance of pH and ionic strength on selectivity of protein fractionation (e.g., Nakao et al., 1988; Zhang and Spencer, 1993; Sudareva et al. 1992; Saksena and Zydney, 1994; van Eijndhoven et al., 1995; Iritani et al., 1995; Ghosh and Cui, 1997).

Another way to interfere with protein–membrane interaction is to modify the membrane surface by chemical and physical methods such as irradiation, synthetic modification, and protein adsorption (e.g., Higuchi et al., 1991; Nakatsuka and Michaels, 1992; Kim and Fane, 1995; Millesime et al., 1996; Ehsani et al., 1997; Ghosh and Cui, 1997).

Bulk mass-transfer limitations have been shown to have a significant effect on flux and selectivity in an ultrafiltration process (e.g., Saksena and Zydney, 1997). To overcome concentration polarization, various techniques for improvement of system hydrodynamics have been investigated. These include vortex mixing (e.g., Belfort et al., 1993; Bellhouse et al., 1994; Balakrishnan and Agarwal, 1996), tube inserts (e.g., Najarian and Bellhouse, 1996), pulsatile flow (e.g., Wang et al., 1994), and gas sparging (e.g., Cui, 1993; Cui and Wright, 1994, 1996; Cabassud et al., 1997; Mercier et al., 1997). Most of the techniques proved effective in enhancing ultrafiltration in terms of increasing the permeate flux. Relatively fewer re-

Correspondence concerning this article should be addressed to Z. Cui.

ports are available on hydrodynamic effect on selectivity of protein fractionation.

The creation of gas–liquid two-phase flow in a membrane module by sparging compressed air has been shown to reduce concentration polarization and fouling in ultrafiltration. The injection of gas bubbles creates bubble-included secondary flow and promotes local mixing near the membrane surface, enhancing the mass transport. The bubbles may also physically remove accumulated solute molecules from the membrane surface. The disruption of concentration polarization will reduce the wall concentration and hence the transmission of the solute. Cui (1993) has reported an increase in rejection coefficient from 0.80 to 0.93 for 87 kDa dextran when using gas sparging during ultrafiltration with a 100-kDa MWCO membrane. Cui and Wright (1996) have also observed a 5–10% increase in rejection coefficient of BSA and dyed dextran to gas sparging during ultrafiltration with the same membrane.

When fractionating a mixture of macromolecules (e.g., proteins) by ultrafiltration, the concentration polarization of the largely rejected molecule is expected to be more severe than that of the more transmitted one. Thus gas sparging will have a greater effect on reducing the wall concentration of the largely rejected species and hence increase the efficiency of fractionation. In the present work, an attempt is made to investigate the effect of gas sparging on fractionation of BSA and lysozyme using a 100-kDa MWCO flat-sheet, polysulfone membrane. The effects of different parameters such as gas flow rate, liquid cross-flow rate, transmembrane pressure, and feed concentration on selectivity of protein fractionation are examined. The possible limitations of gas sparging in ultrafiltration are also discussed.

Experimental Studies

Materials

Lysozyme (from chicken egg white, MW 14,100, pI 11.0) and BSA (bovine serum albumin, MW 67,000, pI 4.9) were purchased from Sigma Chemical Company. All test solutions were prepared using bi-distilled water, further microfiltered through 0.1-micron membrane (Whatman). Polysulfone membrane sheets (PS100, product no. 01110026, MWCO 100 kDa) were purchased from Intersep Ltd., UK. An operating pH of 7.0 and ionic strength of 20 mM phosphate were identified as being suitable for fractionation of BSA and lysozyme using 100 kDa polysulfone membrane.

Apparatus and Procedure

The experimental apparatus is shown in Figure 1. A purpose-built rectangular, flat-sheet, tangential-flow ultrafiltration module was designed, fabricated, and installed vertically. The membrane surface area provided by the module is 5.6 cm × 9.6 cm. The gap of the flow channel is 2 mm. A gear pump (Verder, model 2036 auto) was used to pump the feed solution into the membrane module at the lower end to create an upward crossflow. Two-phase flow was created by injecting compressed air into the feed stream through a T-piece of 6-mm internal diameter. The gas bubbles were distributed throughout the cross section of the flow channel using a distributor at the base of the module. Liquid and gas flow rates

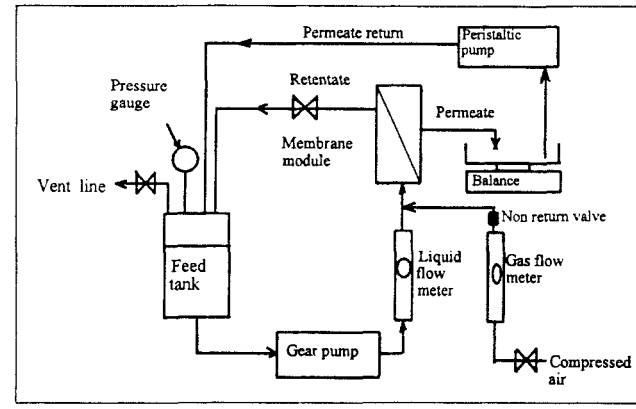

Figure 1. Experimental setup of two-phase flow ultrafiltration rig.

were monitored using rotameters and the gas flow-rate readings were corrected to the corresponding operational pressure. The transmembrane pressure (TMP) is maintained by controlling the exit flow of gas stream from the pressurized feed tank. Permeate collected was periodically recycled back to the reservoir using a peristaltic pump (Watson Marlow 302S) to keep the feed concentration constant. After every operation, the membrane module was cleaned using distilled water followed by detergent (Tergazyme) solution and then thoroughly rinsed using distilled water. Pure water flux was measured to assess the effectiveness of this cleaning procedure prior to the next protein experiment.

Feed and periodically collected permeate samples were analyzed for protein concentration using FPLC (Fast Protein Liquid Chromatography, Pharmacia). An FPLC analytical protocol, based on Superose 6 gel filtration column, was developed for analysis of BSA and lysozyme. The flow rate used was 0.3 mL min^{-1}. The mobile phase used was 20 mM sodium phosphate + 100 mM NaCl, pH 7.0. Prior to injection, the samples were centrifuged at 13,000 rpm for 5 min to get rid of tiny gas bubbles (if any). A 100-μL sample loop was used for sample injection. Calibration curves (AUC_{280} vs. concentration) were prepared for BSA and lysozyme and sensitivity of detection were 0.001 kg·m^{-3} for lysozyme and 0.002 kg·m^{-3} for BSA. The permeate fluxes were determined by weighing the permeate at timed intervals using an electronic balance (Mettler PM 4800).

Parameters for Assessment

The parameters to be considered in ultrafiltration processes are permeate flux (J) and solute rejection or sieving coefficients. The permeate flux is the filtration rate per unit of membrane surface, while the amount of solute going through the membrane may be quantified in terms of the intrinsic rejection coefficient (R_i) or intrinsic sieving coefficient (S_i):

$$R_i = 1 - (C_p/C_w); \qquad S_i = (C_p/C_w). \tag{1}$$

The intrinsic membrane rejection coefficient for a particular membrane-solute system increases with increasing TMP, increasing permeate flux, and higher molecular weights, but is

Table 1. BSA/Lysozyme Fractionation: Effect of Gas Flow Rate

Gas Flow Rate $(m^3 \cdot s^{-1}) \times 10^6$	Permeate Flux $(kg \cdot m^{-2} \cdot s^{-1}) \times 10^2$	S_a for BSA	S_a for Lysozyme	Selectivity (ψ)
0	0.93	0.078	0.846	10.9
1.67	0.96	0.004	0.776	194.0
3.33	0.97	0.004	0.785	196.3
6.67	1.00	0.004	0.739	184.8

Feed = 2 $kg \cdot m^{-3}$ BSA + 2 $kg \cdot m^{-3}$ lysozyme; buffer = 20 mM phosphate, pH 7.0; Membrane = PS 100 kDa MWCO; TMP = 0.5 bar; liquid flow rate = 8.33×10^{-6} $m^3 \cdot s^{-1}$; $u_1 = 0.074$ $m \cdot s^{-1}$.

Table 3. BSA/Lysozyme Fractionation: Effect of Gas Flow Rate

Gas Flow Rate $(m^3 \cdot s^{-1}) \times 10^6$	Permeate Flux $(kg \cdot m^{-2} \cdot s^{-1}) \times 10^2$	S_a for BSA	S_a for Lysozyme	Selectivity (ψ)
0	1.10	0.250	0.904	3.6
0.50	1.19	0.019	0.901	47.4
0.83	1.19	0.014	0.815	58.2
1.67	1.26	0.015	0.810	54.0

Feed = 1 $kg \cdot m^{-3}$ BSA + 1 $kg \cdot m^{-3}$ lysozyme; buffer = 20 mM phosphate, pH 7.0; membrane = PS 100 kDa MWCO; TMP = 0.5 bar; liquid flow rate = 8.33×10^{-6} $m^3 \cdot s^{-1}$; $u_1 = 0.074$ $m \cdot s^{-1}$.

independent of system hydrodynamics (van den Berg et al., (1989). However, a significant change in R_i is observed only when permeate flux or transmembrane pressure is changed by at least one order of magnitude. Therefore, when operating in a narrow permeate flux range, the value of R_i can be considered to be a constant in that range, for all practical purposes.

The solute concentration on the membrane surface, C_w, is difficult to determine experimentally. More practical parameters such as the apparent rejection coefficient, R_a, or the apparent sieving coefficient, S_a, can be used to quantify the proportion of solute crossing the membrane:

$$R_a = 1 - (C_p/C_b); \qquad S_a = (C_p/C_b). \tag{2}$$

The apparent rejection coefficient depends on the hydrodynamics of the membrane module and the feed concentration. Also, R_a first increases and then decreases again when the transmembrane pressure is increased (van den Berg et al., 1989).

For fractionation of a binary mixture of solutes, it is desirable to achieve maximum transmission of one solute and minimum transmission of the other. Efficiency of solute fractionation is expressed in terms of the selectivity, ψ:

$$\psi = (S_{a1})/(S_{a2}). \tag{3}$$

Results and Discussion

Effect of Gas Sparging on Protein Fractionation

Effect of gas flow rate. As is evident from Table 1, gas sparging increases selectivity in protein fractionation. About an 18-fold increase in selectivity was achieved simply by sparging a small amount of gas. The results indicate that increasing the gas flow rate higher than 1.67×10^{-6} $m^3 \cdot s^{-1}$ ($u_g = 0.015$ $m \cdot s^{-1}$) does not result in significant further change in the sieving coefficients of either BSA or lysozyme. This trend is consistent with the observations of earlier workers [Cui, 1993; Cui and Wright, 1994, 1996]. This is possibly due to the fact that in two-phase flow for a given liquid flow rate, local mixing within the module cannot be increased significantly by increasing the gas flow rate. Hence a low gas flow rate could be used in order to achieve significant enhancement in protein fractionation and minimize the risk of foaming and protein denaturation.

Table 2 shows experimental results obtained using the same feed conditions and liquid flow rate but lower TMP (0.3 bar). In single-phase flow, the sieving coefficients for both BSA and lysozyme were lower than those observed at 0.5-bar TMP. This is due to lower concentration polarization. Under these conditions, very low rates of gas sparging are good enough to strip the membrane surface of accumulated solutes. At gas flow rates of 0.83×10^{-6} $m^3 \cdot s^{-1}$ ($u_g = 0.0074$ $m \cdot s^{-1}$) and above, nearly complete separation of BSA and lysozyme was achieved.

Table 3 shows the effect of gas flow rate at lower feed concentration (1 $kg \cdot m^{-3}$ each of BSA and lysozyme), at 0.5-bar TMP. S_a values for both BSA and lysozyme were greater than those observed with higher feed concentrations. Due to the high transmission of BSA, a lower selectivity was observed in the case of single-phase flow ultrafiltration. However, in the case of gas-sparged ultrafiltration, highly enhanced selectivity values were obtained even at very low gas flow rates (e.g., 0.5×10^{-6} $m^3 \cdot s^{-1}$).

The proportional reduction in transmission of BSA due to gas sparging is found to be greater in comparison to that of lysozyme. Thus gas sparging can be utilized to enhance the fractionation of BSA and lysozyme. During ultrafiltration, BSA, which is the larger of the two molecules, is likely to be accumulated near the membrane surface to a much greater extent than lysozyme. Increased local mixing caused by gas sparging results in enhanced back diffusion from the boundary layer and reduces wall concentration of the proteins. This

Table 2. BSA/Lysozyme Fractionation: Effect of Gas Flow Rate

Gas Flow Rate $(m^3 \cdot s^{-1}) \times 10^6$	Permeate Flux $(kg \cdot m^{-2} \cdot s^{-1}) \times 10^2$	S_a for BSA	S_a for Lysozyme	Selectivity (ψ)
0	0.75	0.059	0.780	13.2
0.83	0.78	Undetectable	0.724	Nearly complete separation
1.67	0.82	Undetectable	0.710	Nearly complete separation

Feed = 2 $kg \cdot m^{-3}$ BSA + 2 $kg \cdot m^{-3}$ lysozyme; buffer = 20 mM phosphate, pH 7.0; membrane = PS 100 kDa MWCO; TMP = 0.3 bar; liquid flow rate = 8.33×10^{-6} $m^3 \cdot s^{-1}$; $u_1 = 0.074$ $m \cdot s^{-1}$.

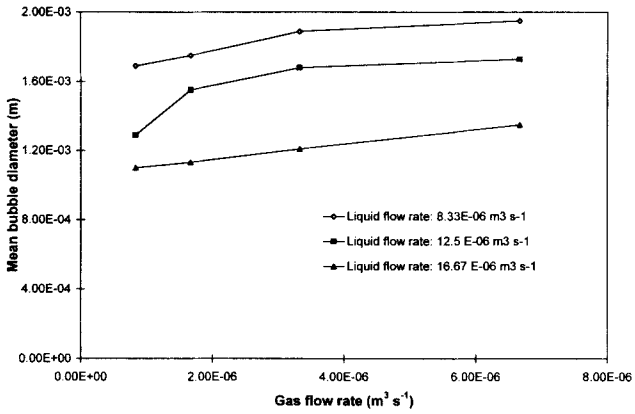

Figure 2. Bubble size at different gas and liquid flow rates.

has a more pronounced effect on the transmission of BSA than that of lysozyme.

High-speed photographs of the bubbles were taken in order to ascertain the average bubble size and distribution under different gas and liquid-flow conditions. It is observed that for a fixed liquid flow rate, if the gas flow rate is increased, there is an increase in the average bubble diameter (Figure 2). The channel width of the module is 2 mm. With bubbles smaller than 2 mm in diameter, the mechanism of reduction in the thickness of the boundary layer is by bubble-induced secondary flow. A rising bubble moves faster than the liquid medium, thereby replacing liquid and creating velocity component perpendicular to the direction of the motion of the bubble. This kind of secondary flow results in generation of a turbulent zone following the bubble that is referred to as the wake. Bubbles larger than 2 mm in diameter (observed in the plane parallel to the membrane surface) will nearly span the entire width of the channel. These bubbles will physically disturb the concentration polarization boundary layer and strip the membrane surface of solute molecules, and also contribute to the reduction in the thickness of the boundary layer by the turbulence generated by their wake. It was observed that bubble size can vary within a certain range, and hence both mechanisms are expected to contribute to the observed experimental results. The liquid Reynolds number (*Re*) within the module when operating at a liquid flow rate of 8.33×10^{-6} m^3 s^{-1} is 286, which is in the laminar range.

The introduction of gas bubbles results in generation of turbulence even at low liquid *Re* values. The effect of gas sparging is, however, expected to be less significant when the liquid flow is already in the turbulent flow regime when bubbles can only increase turbulence to an extent that is far less significant than the flow transition effect (Cui, 1993). Hence gas sparging may not be very effective in modules in which liquid flow is already turbulent or in high shear devices such as hollow fiber and vortex flow units.

It should be pointed out that the enhancement in separation is not due to foam fractionation, as foam fractionation does not take place above a critical protein concentration (Varley et al., 1996). The concentration of BSA and lysozyme in the feed were much higher than their respective critical concentrations.

Effect of Liquid Flow Rate. The effect of liquid flow rate on selectivity of fractionation was examined under single-phase flow conditions, and the effect of gas sparging was studied at these different liquid flows using one particular gas flow rate of 1.67×10^{-6} $m^3\cdot s^{-1}$ ($u_g = 0.015$ $m\cdot s^{-1}$). The results are shown in Table 4. At all the liquid flow rates examined, the single-phase liquid flow within the module is laminar (liquid *Re* ranges from 286 to 572). In single-phase flow, there is a marginal increase in selectivity with increase in the liquid flow rate due to a slight increase in the mass-transfer coefficient. A dramatic increase in the mass-transfer coefficient with an increase in the liquid flow rate is only expected when the liquid flow becomes turbulent. Injecting gas bubbles introduces secondary flow, which outweighs the effect of bulk laminar flow and results in a significant increase in selectivity. With gas sparging at the same gas flow rate an increase in the liquid flow rate results in a lowering of selectivity. This may seem surprising, as at a higher liquid flow rate there is greater bulk flow within the module, and hence a higher velocity gradient is expected at the liquid–wall interface. However, in gas-sparged systems the effect of bubble-induced secondary flow plays a more important role than the bulk fluid flow. The former is heavily dependent on the ratio of volumetric gas flow rate to volumetric liquid flow rate. This phenomenon is discussed in considerable detail in a subsequent section.

Effect of Transmembrane Pressure. Table 5 shows the effect of transmembrane pressure on the fractionation of BSA and lysozyme using single-phase and two-phase flow ultrafiltration. The gas and liquid flow rates were kept fixed at 1.67×10^{-6} $m^3\cdot s^{-1}$ and 8.33×10^{-6} $m^3\cdot s^{-1}$, respectively. The feed concentration was 2 $kg\cdot m^{-3}$ each of BSA and lysozyme, and the buffer was 20 mM phosphate, pH 7.0. The highest selectivity of separation with gas sparging in the experimental range was observed at 0.3 bar. Sieving coefficient values for both BSA and lysozyme increased with TMP to a certain extent in the range of 0.3 bar to 0.5 bar and then decreased with further increase in TMP. This is observed with both single- and two-phase flow operations. In the low TMP range,

Table 4. Effect of Liquid Flow Rate on Fractionation of BSA and Lysozyme

Liquid Flow Rate $(m^3\cdot s^{-1})\times10^6$	Gas Flow Rate $(m^3\cdot s^{-1})\times10^6$	Permeate Flux $(kg\cdot m^{-2}\cdot s^{-1})\times10^2$	S_a for BSA	S_a for Lysozyme	Selectivity(ψ)
8.33	0	0.93	0.078	0.846	10.9
8.33	1.67	0.96	0.004	0.776	194.0
12.50	0	0.94	0.075	0.836	11.15
12.50	1.67	1.00	0.037	0.741	20.03
16.67	0	0.99	0.068	0.819	12.04
16.67	1.67	1.09	0.050	0.736	14.7

Feed = 2 $kg\cdot m^{-3}$ BSA + 2 $kg\cdot m^{-3}$ lysozyme; buffer = 20 mM sodium phosphate, pH 7.0; membrane = PS 100 kDa MWCO; TMP = 0.5 bar.

Table 5. Effect of TMP on Fractionation of BSA and Lysozyme

TMP (bar)	Single-Phase Flow			Two-Phase Flow		
	S_a for BSA	S_a for Lysozyme	ψ	S_a for BSA	S_a for Lysozyme	ψ
0.3	0.059	0.780	13.2	Negligible	0.710	Very high
0.5	0.115	0.846	7.4	0.004	0.776	194.0
0.7	0.037	0.734	19.8	0.019	0.693	36.5
1.0	0.010	0.615	61.5	0.010	0.602	60.2

Feed: 2 kg m^{-3} BSA + 2 kg m^{-3} lysozyme; buffer: 20 mM phosphate, pH 7.0; membrane: PS 100kDa MWCO; liquid flow rate: 8.33×10^{-6} m^3 s^{-1}; gas flow rate (in two-phase flow): 1.67×10^{-6} m^3 s^{-1}.

the concentration polarization is not severe. As the TMP is increased, the wall concentration increases. Therefore a higher transmission of proteins is observed. However, with an increase in the wall concentration there is expected to be an increase in protein adsorption on the membrane surface (isotherm), eventually leading to fouling. Also, within the concentration polarization layer, positively charged lysozyme and negatively charged BSA could form heteroaggregates by Columbic interaction, resulting in reduced transmission of both BSA and lysozyme. Greater heteroaggregation is expected at higher protein concentrations. Another possible mechanism is gel formation at higher TMP values, which might explain why at 1 bar TMP, the transmission figures are almost identical for single- and two-phase flow operations. The contributions of these mechanisms need to be identified and quantified in further study.

Mechanism

Role of the mass-transfer coefficient on Solute Rejection. From the concentration polarization model for partial rejection of solutes,

$$J_v = k_d \ln[(C_w - C_p)/(C_b - C_p)]. \quad (4)$$

Therefore

$$C_w = C_p + (C_b - C_p)\exp(J_v/k_d). \quad (5)$$

This equation can be used to estimate the wall concentration during ultrafiltration.

From Eqs. 1 and 5, one gets

$$R_i = 1 - C_p/[C_p + (C_b - C_p)\exp(J_v/k_d)]. \quad (6)$$

From Eqs. 2 and 6, one gets

$$S_a = (C_p/C_b) = [\exp(J_v/k_d)(1 - R_i)]/[R_i + \exp(J_v/k_d)(1 - R_i)]. \quad (7)$$

For a given membrane–solute system, S_i and hence R_i have been shown to be weak functions of permeate flux (Opong and Zydney, 1991):

$$S_i = [S_\infty \exp(Pe_m)]/[S_\infty + \exp(Pe_m) - 1]. \quad (8)$$

A close examination of this equation shows that in the permeate flux range examined in our experiments, the intrinsic rejection coefficient is remarkably insensitive to change in flux and can be considered to be a constant for each experimental range. From Eq. 7 it is evident that S_a increases with an increase in the value of (J_v/k_d), a dimensionless group referred to as the external Peclet number (Pe) for an ultrafiltration system. Therefore for ultrafiltration processes being operated in a narrow flux range, S_a is expected to decrease with an increase in the value of k_d, and increase with an increase in the value of J_v. The decrease in the sieving coefficient with an increase in k_d is due to enhanced back transport of solutes from the membrane wall, which results in a lowering of the wall concentration of solutes. When the intrinsic rejection ratio is constant, a decrease in C_w would result in a decrease in C_p (Eq. 1). It is also evident that the change in S_a with Pe is more pronounced at lower values of Pe (corresponding to high values of k_d). At higher values of Pe (corresponding to very low k_d), the value of S_a approaches 1. In the experimental data discussed, the change in Pe due to gas sparging is primarily due to the change in the value of k_d, whereas when J_v increases by 5–8%, there is a several-fold increase in k_d as shown in the next section.

Examining the sensitivity of S_a to Pe by differentiating Eq. 7,

$$dS_a/dPe = [(1 - R_i)R_i \exp Pe]/[R_i + (1 - R_i)\exp Pe]^2. \quad (9)$$

The parameter that best describes the proportional change of S_a with Pe is $[1/S_a\ (dS_a/dPe)$. Numerical examination of Eq. 9 shows that the sieving coefficients of solutes having greater R_i values are more sensitive to a change in Pe. Thus, if we have a two-component solute mixture for example, BSA (MW 67,000) and lysozyme (MW 14,100), where BSA is the more rejected species (higher R_i) and lysozyme is the less rejected species (lower R_i), the change in Pe causes a more dramatic change in the transmission of BSA. Therefore the efficiency of solute separation can be enhanced by increasing the bulk mass-transfer coefficient. It should be pointed out that in the preceding analysis, the two solutes are assumed to be noninteracting. In reality, this may not be the case. Nevertheless, such analysis helps in offering a simplified explanation for a rather complex problem.

Effect of Gas Sparging on the Mass-Transfer Coefficient. The effect of gas sparging on the wall mass-transfer coefficient has been discussed by several authors in connection with electrochemical processes (e.g., Sigrist et al., 1979; Sedahmed, 1985; Hosny et al., 1992). The correlations used to estimate the mass-transfer coefficient were developed based on an

analogy study of heat and mass transfer. Sigrist et al. (1993) have examined the effect of superficial gas and liquid velocities on the mass-transfer coefficient in a vertical, rectangular electrochemical cell that is similar in geometry to our ultrafiltration module. It was found that the mass-transfer coefficient (k_d) is a strong function of gas voidage fraction (ϵ). They have proposed a dimensionless equation to correlate the mass-transfer coefficient with the voidage fraction:

$$Sh = 0.19\,(Sc \cdot Ar)^{1/3}, \tag{10}$$

where

$Ar = (d_b^3\, g\Delta\rho)/(\nu^2\rho_\infty)$

$\Delta\rho = (\rho_l - \rho_g)$

$\rho_\infty = (1-\epsilon)\rho_l + \epsilon\rho_g$

$\epsilon = u_g/(u_g + u_l + u_o)$,

where u_o can be calculated using the following correlation (Clift et al., 1978):

$$u_o = [(2.14\,\sigma/\rho_l d_b) + 0.505\,gd_b]^{1/2}. \tag{11}$$

An important observation made by Sigrist et al. (1993) is that k_d is independent of the height and gap of the flow channel.

The mass-transfer coefficient in a single-phase laminar flow can be calculated by using the Graetz-Lévêque correlation:

$$Sh = 1.62\,[Re \cdot Sc.\,(d_{eqv}/l_t)]^{1/3}. \tag{12}$$

For single-phase flow, the value of k_d ranged between 1.1×10^{-6} m·s^{-1} ($u_l = 0.037$ m·s^{-1}) to 1.7×10^{-6} m·s^{-1} ($u_l = 0.148$ m·s^{-1}) for BSA, and 1.7×10^{-6} m·s^{-1} ($u_l = 0.037$ m·s^{-1}) to 2.7×10^{-6} m s^{-1}($u_l = 0.148$ m·s^{-1}) for lysozyme, depending on the liquid flow rate. The increase of k_d with the liquid flow rate is not very significant in the experimental range, but injection of gas bubbles results in a dramatic increase in k_d, as shown in Figure 3. In the experimental range for two-phase flow, the k_d for BSA ranged between 6.0×10^{-6} m s^{-1} and 6.3×10^{-6} m·s^{-1}, while that of lysozyme ranged between 9.5×10^{-6} m·s^{-1} and 10.0×10^{-6} m·s^{-1}, depending on gas and liquid flow rates. Figure 3 also shows that with gas sparging, the mass-transfer coefficient is not sensitive to the gas flow rate.

The preceding analysis can be used to explain the results shown in Tables 1–4. Gas sparging results in a big increase in k_d, and hence a significant increase in selectivity, when compared with single-phase flow. However, in gas-sparged ultrafiltration, k_d is not very sensitive to the superficial gas velocity, and hence increasing the gas flow rate has little effect. At constant gas flow rate, an increase in the liquid flow rate leads to a reduction in the voidage fraction, and hence the mass transfer coefficient, which reduces selectivity, as shown in Table 4.

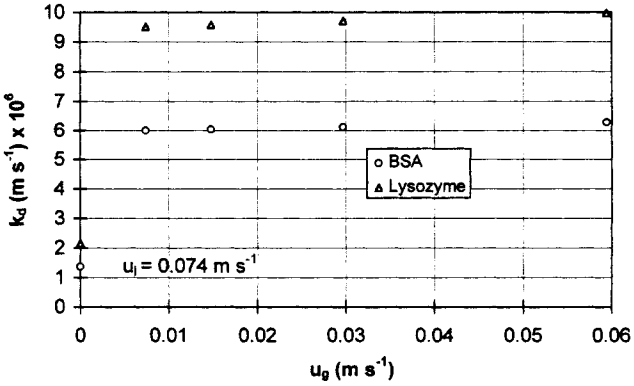

Figure 3. Effect of gas flow rate on mass transfer coefficient.

Gas sparging increases both J_v and k_d. An increase in J_v tends to increase the sieving coefficient, while an increase in k_d has the opposite effect. However, while J_v is found to increase by 5–8%, the increase in k_d is greater than 450%. Hence the net effect of gas sparging is the overwhelming decrease in the sieving coefficient (see Tables 1–4).

It should be emphasized that our experiment only examined the low liquid *Re* range. Also the shear rate on the membrane surface is low, as shown by the mass-transfer coefficient values for single-phase flow. Gas sparging has a dramatic effect in increasing the k_d in the low liquid *Re* range. In high shear membrane modules and in turbulent flow, the k_d in single-phase flow could be much higher. The effect of bubble-induced secondary flow in terms of relative increase in k_d is expected to be less significant.

Bubble Damage to Proteins

Wright and Cui (1994) and more recently Todd et al. (1997) have conducted detailed studies on bubble-induced damage to proteins (e.g., BSA, lysozyme, pepsin, catalase, IgG, and YADH). Techniques such as enzyme assay, oxidation assay, and gel electrophoresis were used in such studies. Sparging at a low gas flow rate causes insignificant damage to proteins, and the extent of damage at high gas flow rate depends on the type of proteins and solution conditions (e.g., pH, ionic strength, concentration). Protein denaturation was mainly found to occur due to secondary or tertiary structure change resulting from the unfolding of proteins at the gas liquid interface and due to substantial shearing when bubbles burst. Denaturation due to oxidation was found to be negligible.

In the gas-sparged ultrafiltration experiments discussed in the present report, the gas flow rates and exposure times are far less than the vigorous conditions studied by Todd et al. (1997). When the extent of foaming is negligible (as observed at low gas flow rates), the extent of protein damage is expected to be insignificant. Tests carried out at high gas flow rates did show a significant foaming problem, and protein damage cannot be neglected in such cases.

Conclusion

The results and observations from this study can be summarized as follows:

1. Gas sparging can enhance protein fractionation. The injection of gas bubbles results in the decrease of transmission of both BSA and lysozyme. The transmission of BSA decreases quite dramatically in gas-sparged ultrafiltration, while with lysozyme this reduction is not so significant.

2. Significant increase in selectivity was observed at low gas flow rates, and the selectivity is found to be insensitive to a further increase in the gas flow rate.

3. Enhancement in selectivity of separation can be explained in terms of the enhancement of bulk mass-transfer coefficient.

4. The low gas flow rate necessary to achieve significant enhancement of selectivity does not cause significant foaming and denaturation of the proteins being fractionated.

Acknowledgment

This project is sponsored by the Biotechnology and Biological Science Research Council UK (GR SPC 05236). One of the authors (R. G.) is grateful to the Association of Commonwealth Universities for financial assistance (Commonwealth Scholarship). The authors thank J. Todd for helping with the bubble damage studies.

Notation

Ar = Arrhenius number ($= d_b^3 g \Delta\rho)/\nu^2\rho_\infty$) (dimensionless)
C_b = concentration of solute in the feed (kg m^{-3})
C_p = concentration of solute in the permeate (kg m^{-3})
d_b = bubble diameter (m)
d_{equ} = equivalent hydraulic diameter of the flow channel (m)
D = diffusivity of solute ($m^2 \cdot s^{-1}$)
D_{eff} = effective diffusivity within the pores ($m^2 \cdot s^{-1}$)
g = acceleration due to gravity ($m \cdot s^{-2}$)
J_v = volumetric permeate flux ($m \cdot s^{-1}$)
l_t = length of membrane module (m)
Pe_m = membrane internal Peclet number ($= S_\infty J_v \delta_m / D_{\text{eff}}$) (dimensionless)
S_{a1} = sieving coefficient of less rejected solute (dimensionless)
S_{a2} = sieving coefficient of more rejected solute (dimensionless)
S_∞ = asymptotic value of the sieving coefficient (dimensionless)
Sc = Schmidt number ($= \nu/D$) (dimensionless)
Sh = Sherwood number ($k_d/d_b D$) (dimensionless)
u_g = superficial gas velocity within the module ($m \cdot s^{-1}$)
u_l = superficial liquid velocity within the flow channel ($m \cdot s^{-1}$)
u_o = rising (terminal) velocity of a rising bubble ($m \cdot s^{-1}$)
δ_m = membrane thickness (m)
μ_l = viscosity of the liquid (Pa·s)
ν = kinematic viscosity ($m^2 \cdot s^{-1}$)
ρ_g = gas density ($kg \cdot m^{-3}$)
ρ_l = density of the liquid ($kg \cdot m^{-3}$)
ρ_∞ = average density ($kg \cdot m^{-3}$)
σ = surface tension ($N \cdot m^{-1}$)

Literature Cited

Balakrishnan, M., and G. P. Agarwal, "Protein Fractionation in a Vortex Flow Filter. I: Effect of System Hydrodynamics and Solution Environment on Single Protein Transmission," *J. Memb. Sci.*, **112**, 47 (1996).

Belfort, G., J. M. Pimbley, A. Greiner, and K. Y. Chung, "Diagnosis of Membrane Fouling Using a Rotating Annular Filter: 1. Cell Culture Media," *J. Memb. Sci.*, **77**, 1 (1993).

Bellhouse, B. J., I. J. Sobey, S. Alani, and B. M. DeBlois, "Enhanced Filtration Using Flat Membranes and Standing Vortex Waves," *Bioseparation*, **4**, 127 (1994).

Cabassud, C., S. Laborie, and J. M. Laiñe, "How Slug Flow Can Improve Ultrafiltration Flux in Organic Hollow Fibres," *J. Memb. Sci.*, **128**, 93 (1997).

Clift, R., J. R. Grace, and M. E. Weber, *Bubbles Drops and Particles*, Academic Press, New York, p. 172 (1978).

Cui, Z. F., "Experimental Investigation on Enhancement of Crossflow Ultrafiltration with Air Sparging," *Effective Membrane Processes - New Perspectives*, R. Patterson, ed., Mechanical Engineering, London, p. 237 (1993).

Cui, Z. F., and K. I. T. Wright, "Gas-Liquid Two Phase Flow Ultrafiltration of BSA and Dextran Solution," *J. Memb. Sci.*, **90**, 183 (1994).

Cui, Z. F., and K. I. T. Wright, "Flux Enhancement with Gas Sparging in Downwards Crossflow Ultrafiltration: Performance and Mechanism," *J. Memb. Sci.*, **117**, 109 (1996).

Ehsani, N., S. Parkkinen, and M. Nyström, "Fractionation of Natural and Model Egg-White Protein Solutions with Modified and Unmodified Polysulfone UF Membranes," *J. Memb. Sci.*, **123**, 105 (1997).

Ghosh, R., and Z. F. Cui, "Fractionation of BSA and Lysozyme Using Ultrafiltration: Effect of pH and Membrane Surface Pretreatment," *J. Memb. Sci.*, in press (1997).

Higuchi, A., S. Mishima, and T. Nakagaya, "Separation of Proteins by Surface Modified Polysulfone Membranes," *J. Memb. Sci.*, **57**, 175 (1991).

Hosny, A. Y., T. J. O'Keffe, J. W. Johnson, and W. J. James, "Effect of Gas Sparging on Mass Transfer in Zinc Electrolytes," *J. Appl. Electrochem.*, **22**, 596 (1992).

Iritani, E., Y. Mukai, and T. Murase, "Upward Dead-End Ultrafiltration of Binary Protein Mixtures," *Sep. Sci. Technol.*, **30**, 369 (1995).

Kim, K. J., and A. G. Fane, "Performance Evaluation of Surface Hydrophilized Novel Ultrafiltration Membranes Using Aqueous Proteins," *J. Memb. Sci.*, **99**, 149 (1995).

Mercier, M., C. Fonade, and C. Lafforgue-Delorme, "How Slug Flow Can Enhance the Ultrafiltration Flux in Mineral Tubular Membranes," *J. Memb. Sci.*, **128**, 103 (1997).

Millesime, L., J. Dulien, and B. Chaufer, "Fractionation of Proteins with Modified Membranes," *Bioseparation*, **6**, 135 (1996).

Najarian, S., and B. J. Bellhouse, "Enhanced Microfiltration of Bovine Blood Using a Tubular Membrane with Screw-Threaded Insert and Oscillatory Flow," *J. Memb. Sci.*, **112**, 249 (1996).

Nakao, S., H. Osada, H. Kurata, T. Tsuru, and S. Kimura, "Separation of Proteins by Charged Ultrafiltration Membranes," *Desalination*, **70**, 191 (1988).

Nakatsuka, S., and A. S. Michaels, "Transport and Separation of Proteins by Ultrafiltration Through Sorptive and Non-Sorptive Membranes," *J. Memb. Sci.*, **69**, 189 (1992).

Opong, W. S., and A. L. Zydney, "Diffusive and Convective Protein Transport Through Asymmetric Membranes," *AIChE J.*, **37**, 1497 (1991).

Rodgers, V. G. J., and R. E. Sparks, "Reduction of Membrane Fouling in Ultrafiltration of Binary Protein Mixtures," *AIChE J.*, **37**, 1517 (1991).

Saksena, S., and A. L. Zydney, "Effect of Solution pH and Ionic Strength on the Separation of Albumin from Immunoglobulins (IgG) by Selective Filtration," *Biotechnol. and Bioeng.*, **43**, 960 (1994).

Saksena, S., and A. L. Zydney, "Influence of Protein-Protein Interactions on Bulk Mass Transport during Ultrafiltration," *J. Memb. Sci.*, **125**, 93 (1997).

Sedahmed, G. H., "A Model for Correlating Mass-Transfer Data in Parallel Plate Gas Sparged Electrochemical Reactors," *J. Appl. Electrochem.*, **15**, 777 (1985).

Sigrist, L., O. Dossenbach, and N. Ibl, "Mass Transport in Electrolytic Cells with Gas Sparging," *Int. J. Heat Mass Transfer*, **22**, 1393 (1979).

Sudareva, N. N., O. I. Kurenbin, and B. G. Belenkii, "Increase in the Efficiency of Membrane Fractionation," *J. Memb. Sci.*, **68**, 263 (1992).

Todd, J. R., R. C. Darton, and Z. F. Cui, "Investigation of Protein Denaturation in Foam Using a Bubble Column," The 1997 Jubilee Research Event, Vol. 2, IChemE, Rugby, U.K., 957 (1997).

van den Berg, G. B., I. G. Racz, and C. A. Smoulders, "Mass Transfer Coefficients in Cross-Flow Ultrafiltration," *J. Memb. Sci.*, **47**, 25 (1989).

van Eijndhoven, R. H. C. M., S. Saksena, and A. L. Zydney, "Protein Fractionation using Electrostatic Interactions in Membrane Filtration," *Biotechnol. Bioeng.*, **48**, 406 (1995).

Varley, J., A. Kaul, and S. Ball, "Partition of Protein from Binary-Mixtures by Batch Foaming Process," *Biotechnol. Tech.*, **10**, 133 (1996).

Wang, Y. Y., J. A. Howell, R. W. Field, and D. X. Wu, "Simulation of Cross-Flow Filtration for Baffled Tubular Channels and Pulsatile Flow," *J. Memb. Sci.*, **95**, 243 (1994).

Wright, K. I. T., and Z. F. Cui, "Identification of Enzyme Activity Loss Caused by Gas Bubbles," *Separations for Biotechnology 3*, D. L. Pyle, ed., Royal Society for Chemistry, London, p. 579 (1994).

Zhang, L., and H. G. Spencer, "Selective Separation of Proteins by Microfiltration with Formed-in-Place Membranes," *Desalination*, **90**, 137 (1993).

Manuscript received May 5, 1997, and revision received Sept. 8, 1997.